Be Star Inclination Angles Derived from Hα Line Profile Fitting

T. A. A. Sigut[1,2], A. K. Mahjour[1] and C. Tycner[3]

1. Department of Physics & Astronomy, The University of Western Ontario, London, Ontario, Canada
2. Western Institute for Earth & Space Exploration, The University of Western Ontario, London, Ontario, Canada
3. Department of Physics, Central Michigan University, Mt Pleasant, Michigan, USA

We show that reliable estimates of the angle between a star's rotation axis and the line-of-sight (the stellar inclination angle) can be efficiently determined for Be stars via Hα emission-line profile modelling. Using a sample of eleven Be stars with available optical interferometry from the Naval Precision Optical Interferometer (NPOI), we compare stellar inclinations angles derived from fitting Hα line profiles to inclinations derived from the major and minor axes of the Be star disk light distributions on the sky. The differences between these two methods are consistent with a normal distribution of a mean of zero and a standard deviation of 7°. As Be stars comprise approximately one-fifth of all upper-main sequence B stars, the Hα profile fitting method is an efficient method for detecting correlated rotation axis in young, open clusters. In addition, the combination of a measured inclination angle and a polarization position angle (that constrains the orientation of the disk's major axis on the sky) can be used to reconstruct the 3D direction of a Be star's rotation axis.

1 Introduction

A Be star is a rapidly-rotating, B-type, main sequence star surrounded by an equatorial, circumstellar disk. The most likely disk formation mechanism involves episodes of near critical rotation of the central B star in which material is ejected from the stellar equator into a disk (Granada et al., 2013); the disk then spreads outward by the action of turbulent viscosity, forming a viscous decretion disk (Rivinius et al., 2013). The defining observational characteristic of a Be star is that its spectrum shows (or has shown in the past) emission in the hydrogen Balmer series, most notably in Hα at $\lambda = 6562.8\,\text{Å}$ (Slettebak, 1982). It has long been known that the morphology of the Hα emission line reflects the inclination angle, $i_\star$, between the common star-disk rotation axis and the line of sight (Porter & Rivinius, 2003). Physically identical Be stars can show a wide range of Hα emission line profiles, from singly-peaked emission for $i_\star \approx 0°$ (pole-on star and face-on disk), to doubly-peaked emission for intermediate $i_\star$, to doubly-peaked emission with strong central, shell absorption for $i_\star \approx 90°$ (equator-on star and edge-on disk). This suggests that detailed profile fitting of the Hα emission line based on radiative transfer modelling may be able to extract a reliable measure of the stellar inclination angle.

Stellar rotation axes are usually assumed to be randomly oriented in space, and therefore a distant observer will measure inclination angles $i_\star$ that satisfy a $\sin i_\star$ distribution (Gray, 1992). As it is difficult to measure $i_\star$ for an individual star (see below), the $\sin i_\star$ distribution is usually assumed and then used to derive other quantities for populations of stars, such as the distribution of stellar equatorial speeds.

Nevertheless, most, and perhaps all, early-type stars are born in clusters, and it is not obvious that the individual stellar spins will be completely randomized during cluster formation. Numerical simulations (Rey-Raposo & Read, 2018) suggest that strongly-aligned stellar spins can result if more than $\approx 40\%$ of the initial kinetic energy of the parent molecular cloud is in the form of rotation. Therefore, observational constraints on the degree of spin alignment (or lack thereof) in young, open clusters may provide important constraints on the interplay of gravitation, turbulence and magnetic fields during cluster formation.

As noted above, it is difficult to determine the inclination angle of a single star. However, there are some possible approaches:

- Measurement of the projected equatorial rotational speed ($v \sin i_\star$) from the broadening of spectral lines plus an estimate of the star's underlying rotation period from photometric or magnetic variations can be used to extract $i_\star$ (Abt, 2001, for example).
- Very rapid stellar rotation leads to gravitational darkening in which the star becomes oblate with a temperature variation over it's surface (Collins, 1965). As the star's spectrum now depends on how it is viewed, an estimate of $i_\star$ can be extracted from careful spectral synthesis. As Be stars are known rapid-rotators, this technique is applicable (Frémat et al., 2005; Zorec et al., 2016).
- Another approach is the use of asteroseismology in which the relative power in rotationally-split, azimuthal modes corresponding to a given angular degree can be used to measure the inclination (Gizon & Solanki, 2003). Using this method, Corsaro et al. (2017) have recently detected the first observational evidence of strong spin alignment among red giants in two, old Galactic open clusters, NGC 6791 and NGC 6819, based on three years of *Kepler* data.

Nevertheless, all three of these methods are data intensive and require extensive time series and/or high signal-to-noise observations. In this work, we propose a simpler method overcoming these limitations based on the spectra of Be stars in which a single Hα observation of moderate resolution ($\mathcal{R} \equiv \lambda/\Delta\lambda \approx 10^4$) and signal-to-noise ($S/N \approx 10^2$) can yield a reliable estimate of $i_\star$.

2 Hα Line Profile Libraries

As the heart of the method to determine $i_\star$ proposed in this work is Hα line profile fitting, we have used the `Beray` code (Sigut, 2011, 2018) to compute theoretical Hα profiles for a large number of Be star models. The circumstellar disk density was taken to fall with radius as a power-law of index n, starting from a value ρ_0 at the stellar surface. The thermal structure of the circumstellar disk was determined using the `Bedisk` code (Sigut & Jones, 2007; Sigut, 2018) which enforces radiative equilibrium in a gas of solar chemical composition heated by the photoionizing radiation appropriate to the spectral type of the central B star. For each spectral type, the Hα line profile is a function of four model parameters: the base disk density, ρ_0 (range 10^{-12} to 10^{-10} gm cm^{-3}), the power-law index, n (range 1.5 to 4.0), the outer disk radius, R_d (range 5 to 65 $\mathrm{R}_\odot$), and the system viewing inclination, $i_\star$ (range 0° to 90°). Models were computed for eleven spectral types between B0 and B9, making a total Hα library of over 231,000 profiles.

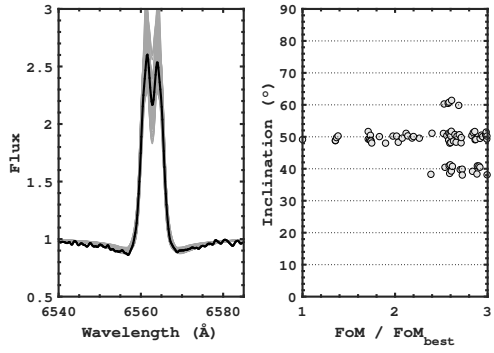

Fig. 1: Left: A simulated Hα line profile (solid back line) with $S/N = 10^2$ and resolution $\mathcal{R} = \lambda/\Delta(\lambda) = 10^4$ corresponding to spectral type B6 and model parameters $\rho_0 = 7.69 \times 10^{-11}$ g cm^{-3}, $n = 3.0$, $R_d = 25\,R_*$, and $i_\star = 50°$. The light grey lines are all model profiles that fit within a factor of 3 of the best fit profile. Right: The inclination distribution of model profiles shown in the left panel.

To extract $i_\star$ for a Be star, it's observed Hα line profile is compared to each model profile in the line library of the appropriate spectral type. The model with the minimum figure-of-merit, taken to be the average absolute percentage difference between the observed relative flux profile and the model profile, defines the disk parameters (ρ_0, n, R_d) and inclination angle $i_\star$ that best represents the star.

One important issue is that there may be degeneracies among the parameters such that wide range of inclinations $i_\star$ may fit the observed profile equally well by adjusting the values of the disk density parameters $(\rho_0, n, R_\mathrm{d})$. We tested this issue extensively via Monte Carlo simulation and find that while such degeneracies do exits, the distribution in inclination of the best-fitting profiles is small, $\Delta\, i \leq 10°$ even if large uncertainties in the the assigned spectral types are included.

Figure 1 illustrates one such simulated profile fit and the distribution in recovered $i_\star$. The simulated observed Hα profile was generated with $S/N = 10^2$ and resolution $\mathcal{R} = 10^4$, both typical of Be star observations. The fitting models shown in this figure are all those fitting within a factor of three of the best-fitting model, i.e. if $\mathcal{F}_\mathrm{min}$ is the figure-of-merit of the best-fit profile, then all models with $\mathcal{F} \leq 3\,\mathcal{F}_\mathrm{min}$ are shown. Note that this is a very generous limit and includes many profiles that visually do not fit the target profile. Despite this, the target inclination of $i_\star = 50°$ is robustly recovered.

3 The NPOI Interferometric Sample

To observationally test how the proposed Hα profile-fitting method performs, we assembled a sample of eleven Be stars with published interferometric visibilities from the Naval Precision Optical Interferometer (Armstrong et al., 1998). Interferometric observations resolve the Be star disk light distribution on the sky, and a geometric model of a circular star plus an elliptical Gaussian disk (Tycner et al., 2003) can be fit to the observed visibilities (which are the Fourier transform of the light distribution). The four fit parameters in this model are: the disk major axis (a), the disk minor axis

Tab. 1: The Be stars in the NPOI sample

Stellar Parameters				Interferometry		
Name	HD	Spectral Type	Distance (pc)	N_{V^2}	$r = b/a$	ϕ (°)
γ Cas	5394	B0.5IV	188	169	0.621 ± 0.044	32 ± 2
ϕ Per	10516	B1.5V	221	186	0.275 ± 0.010	118 ± 1
ψ Per	22192	B5Ve	179	387	0.323 ± 0.016	133 ± 1
η Tau	23630	B7III	124	300	0.839 ± 0.030	40 ± 10
48 Per	25940	B3Ve	146	291	0.707 ± 0.038	122 ± 5
β CMi	58715	B8Ve	49	720	0.695 ± 0.112	140 ± 25
κ Dra	109387	B6IIIe	140	276	0.596 ± 0.065	120 ± 5
χ Oph	148184	B2Vne	150	132	0.663 ± 0.187	121 ± 31
υ Cyg	202904	B2Vne	187	201	0.889 ± 0.060	184 ± 51
o Aqr	209409	B7IVe	134	994	0.251 ± 0.086	113 ± 4
β Psc	217891	B6Ve	130	200	0.810 ± 0.073	133 ± 30

(b), the position angle of the major axis on the sky (χ), and a brightness ratio between the disk and the central star (c_*). As Be star disks are equatorial and circular, the observed axial ratio is due to projection through the stellar inclination angle, i.e. $r \equiv b/a = \cos i_\star$; hence, the system inclination can be recovered geometrically from the interferometric observations in a manner independent of any radiative transfer modelling. Of course, the simple relation $r = \cos i_\star$ must fail for sufficiently large $i_\star$ as the minor axis will be limited by the disk's finite scale height; however, simulated Hα images computed with `Beray` suggest this occurs only for $i > 80°$ due to the thinness of Be star disks (Sigut et al., 2009).

Table 1 lists the 11 Be stars that form our observational sample. Given in the table are the stellar particulars (spectral type and distance) as well as the results of the interferometric modelling. Errors in the axial ratio and disk position angle are determined via bootstrap Monte Carlo simulations (Wall & Jenkins, 2003), based on 500 random realizations of the visibility data. References for the interferometric data are: γ Cas (Tycner et al., 2003); η Tau, β CMi (Tycner et al., 2005); ϕ Per (Tycner et al., 2006); κ Dra, υ Cyg, β Psc (Jones et al., 2008); χ Oph (Tycner et al., 2008), o Aqr (Sigut et al., 2015), 48 Per (Jones et al., 2017), and ϕ Per (Sigut *et al.* 2020, private communication). Observed Hα line profiles were taken from observations at the John S. Hall telescope at Lowell Observatory, and all spectra have $S/N = 10^2$ and $\mathcal{R} = 10^4$.

Fits to the eleven observed Hα line profiles, along with the best-fitting disk parameters and inclinations, are shown in Fig. 2. The fits are generally good; however, in some cases (ϕ Per, for example) there is a systematic difference between the available models and the observations. In addition, the profiles in this sample are nearly symmetric, whereas many Be stars show asymmetric profiles with V/R variations, i.e. sizable differences between the height of the red (R) and blue (V) emission peaks. In tests, we have had success in fitting the red and blue sides of asymmetric Hα profiles separately, extracting a consistent $i_\star$ from both fits; however, this is outside the scope of the current project.

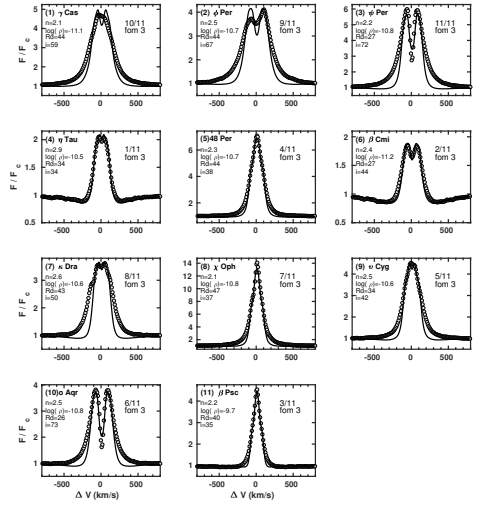

Fig. 2: Hα line profile fits (solid black lines) to the observed NPOI sample profiles (circles). Parameters for the best-fitting model for each star are given in the panels. Each fit is ranked; for example, the fit for *o* Aqr is 6/11, i.e. the 6th best fit out of 11.

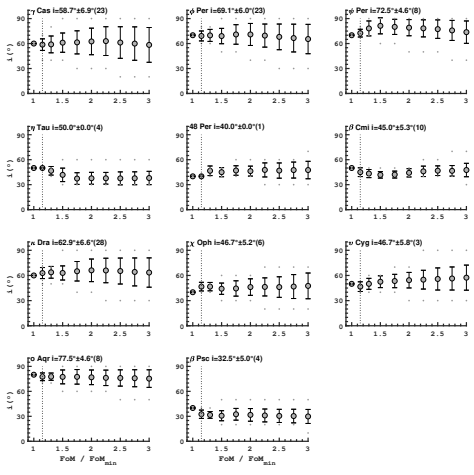

Fig. 3: The average inclination and standard deviation of all models that fit each NPOI sample profile to within a given figure-of-merit. The error bars are 1σ and the dots above and below give the minimum and maximum inclinations obtained.

Figure 3 shows how the recovered inclination changes for each sample star as fits with larger figures-of-merit $\mathcal{F}$ are considered. Shown is the mean $i_\star$, its standard deviation, and the minimum and maximum inclinations, as a function of $\mathcal{F}/\mathcal{F}_{\rm min}$ of the fits. For example, when $\mathcal{F}/\mathcal{F}_{\rm min} = 2$, all model profiles that fit within a factor of 2 of the figure-of-merit of the best-fitting profile are considered when determining the mean $i_\star$ and its standard deviation. As can be seen from the figure, the inclination recovered from Hα line profile fitting is fairly insensitive to cut-off in $\mathcal{F}/\mathcal{F}_{\rm min}$. This reflects the fact that the profile shape is generally more sensitive to $i_\star$ than the three disk density parameters (Sigut et al., 2015).

Figure 4 compares the inclination angle determined from Hα profile fitting (Fig. 2) with the inclination determined from interferometric models (Tab. 1) for the 11 NPOI sample stars. The linear correlation coefficient between these two methods exceeds 0.9. The difference between the spectroscopic inclinations and interferometric inclinations is consistent with a normal distribution of a mean of $\mu = -1°$ and a standard deviation of $\sigma = 7°$. Thus, based on this sample, stellar inclinations of an accuracy of $\approx \pm 10°$ are obtainable from Hα line profile fitting.

4 Polarization

The inclination angle of a star constrains the stellar rotation axis to lie along a cone of opening angle $i_\star$ with respect to the observer's line of sight. In the case of interferometric observations, we also have the positional angle of the major axis of the equatorial disk on the sky; the combination allows us to reconstruct the 3D orientation of the stellar rotation axis in space. While interferometric observations

that resolve the disk are currently only possible for the nearest Be stars, continuum polarization measurements offer a proxy for the disk's position angle. The continua of Be stars are known to be weakly polarized (Yudin, 2001). This polarization is naturally explained by the scattering of stellar light by the flattened, circumstellar disk (Poeckert & Marlborough, 1977). The position angle of the net polarization vector should be perpendicular to the scattering plane, i.e. the circumstellar disk, aligned with the projected stellar rotation axis on the sky. We can test this simple prediction for our NPOI sample of Be stars by following Quirrenbach et al. (1997) and comparing the polarization position angle, ϕ, given by Yudin (2001) for each star with $\chi + 90^\circ$ where χ is the interferometric position angle of Tab. 1. The result can be seen in Fig. 5. As there is an 180° ambiguity in both of these angles, they are represented in Fig. 5 in the unit circle.

As can be seen from Fig. 5, five of eleven stars have agreement of ϕ and $\chi + 90^\circ$ to within the interferometric uncertainties, and an additional three are close and likely agree for any reasonable errors in the polarization position angles. However, there are three significant disagreements: β Psc, η Tau and 48 Per, and in these cases, the angle $\chi + 90^\circ$ seems perpendicular to the disk. The misalignment in the case of 48 Per was first reported by (Delaa et al., 2011) and is discussed by Rivinius et al. (2013), who caution that the small intrinsic polarization expected from 48 Per makes it difficult to separate from the much larger interstellar contribution. Without uncertainties in the polarization position angles, however, it is hard to evaluate the statistical significance of these three (out of 11) apparently perpendicular angles.

5 Discussion

We demonstrate that a single Be star Hα emission-line profile of moderate signal-to-noise and resolution can be used to determine the inclination angle of the central B-type star to within $\approx \pm 10^\circ$. As Be stars comprise upwards of one-fifth of all main sequence B-type stars (Zorec & Briot, 1997), Be stars provide a promising avenue to look for possible spin-correlations between massive stars in young open clusters. We also suggest that Hα profile fitting to determine $i_\star$ combined with polarization measurements for Be stars will allow the reconstruction of the 3D orientation of the central B star's rotational axis.

We are currently extended our method to include Hβ, also often observed in emission in Be stars, and extending our method to deal with the numerous Be stars that exhibit asymmetric Hα emission-line profiles.

Acknowledgements. T. A. A. S. acknowledges support from the Natural Sciences and Engineering Council of Canada through a Discovery Grant. C. T. acknowledges support from the National Science Foundation through grant AST-1614983. The Navy Precision Optical Interferometer is a joint project of the Naval Research Laboratory and the U.S. Naval Observatory, in cooperation with Lowell Observatory, and is funded by the Office of Naval Research and the Oceanographer of the Navy. We thank the Lowell Observatory for the telescope time used to obtain the Hα spectra used in this work.

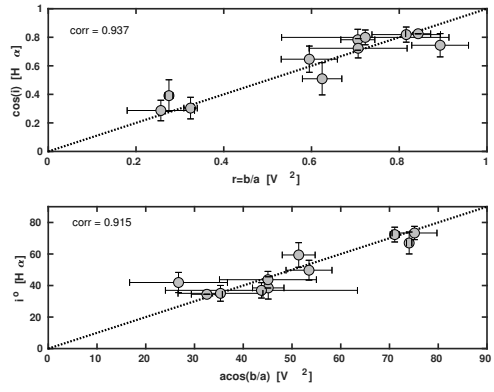

Fig. 4: Comparison of the spectroscopic and interferometric inclinations for the eleven stars in the NPOI sample. In the top panel, the spectroscopic inclination angles are converted to axial ratios using $\cos(i_{H\alpha})$. In the bottom panel, the interferometric axial ratios are converted to inclination angles via $i_{V^2} \equiv \cos^{-1}(b/a)$. Errors in $i_{H\alpha}$ are defining using all models satisfying $\mathcal{F}/\mathcal{F}_{\rm min} \leq 1.15$. Errors in the interferometric inclination angles follow from the errors in the major and minor axes of Tab. 1. The lines in each panel are of unit slope and the linear correlation coefficient is indicated in each panel.

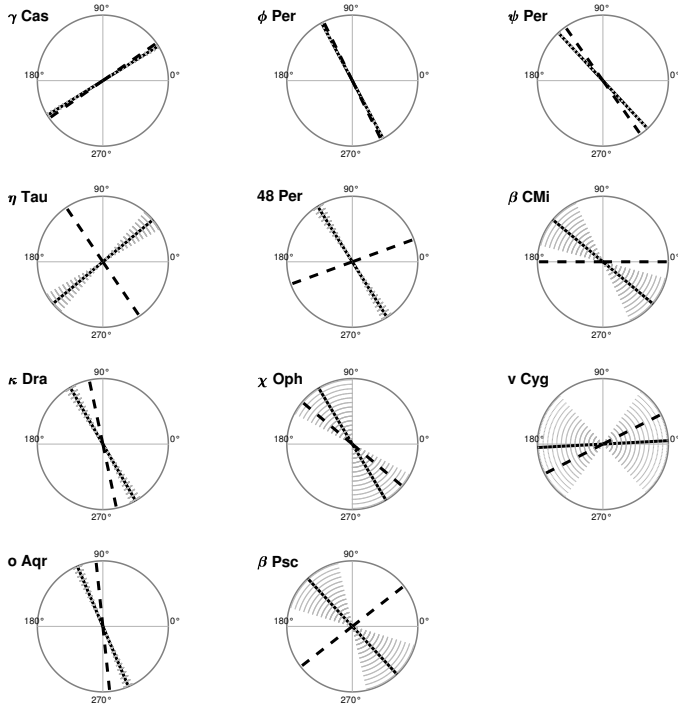

Fig. 5: Comparison of the polarization position angle of Yudin (2001) (dotted line) with the disk's major axis position angle +90° (solid line) for the eleven NPOI sample stars. The shaded area reflects the major axis position angle uncertainty of Tab. 1.

References

Abt, H. A., *AJ* **122**, 2008 (2001)

Armstrong, J. T., et al., *ApJ* **496**, 1, 550 (1998)

Collins, G. W., II, *ApJ* **142**, 265 (1965)

Corsaro, E., et al., *Nature Astronomy* **1**, 0064 (2017)

Delaa, O., et al., *A&A* **529**, A87 (2011)

Frémat, Y., Zorec, J., Hubert, A.-M., Floquet, M., *A&A* **440**, 305 (2005)

Gizon, L., Solanki, S. K., *ApJ* **589**, 2, 1009 (2003)

Granada, A., et al., *A&A* **553**, A25 (2013)

Gray, D. F., The Observation and Analysis of Stellar Photospheres, Cambridge University Press, The Pitt Building, Trumpington Street, Cambridge, UK, 2 edition (1992)

Jones, C. E., et al., *ApJ* **687**, 598 (2008)

Jones, C. E., et al., *ApJ* **843**, 24 (2017)

Poeckert, R., Marlborough, J. M., *ApJ* **218**, 220 (1977)

Porter, J. M., Rivinius, T., *PASP* **115**, 1153 (2003)

Quirrenbach, A., et al., *ApJ* **479**, 1, 477 (1997)

Rey-Raposo, R., Read, J. I., *MNRAS* **481**, 1, L16 (2018)

Rivinius, T., Carciofi, A. C., Martayan, C., *A&A Rev.* **21**, 69 (2013)

Sigut, T. A. A., in C. Neiner, G. Wade, G. Meynet, G. Peters (eds.) IAU Symposium, *IAU Symposium*, volume 272, 426 (2011)

Sigut, T. A. A., in Workshop on Astrophysical Opacities, *Astronomical Society of the Pacific Conference Series*, volume 515, 213 (2018)

Sigut, T. A. A., Jones, C. E., *ApJ* **668**, 481 (2007)

Sigut, T. A. A., McGill, M. A., Jones, C. E., *ApJ* **699**, 1973 (2009)

Sigut, T. A. A., Tycner, C., Jansen, B., Zavala, R. T., *ApJ* **814**, 159 (2015)

Slettebak, A., in M. Jaschek, H.-G. Groth (eds.) Be Stars, *IAU Symposium*, volume 98, 109–121 (1982)

Tycner, C., et al., *AJ* **125**, 3378 (2003)

Tycner, C., et al., *ApJ* **624**, 359 (2005)

Tycner, C., et al., *AJ* **131**, 5, 2710 (2006)

Tycner, C., et al., *ApJ* **689**, 461 (2008)

Wall, J. V. W., Jenkins, C. R. J., Practical Statistics for Astronomers, Cambridge University Press, The Edinburgh Building, Cambridge, UK, 1 edition (2003)

Yudin, R. V., *A&A* **368**, 912 (2001)

Zorec, J., Briot, D., *A&A* **318**, 443 (1997)

Zorec, J., et al., *A&A* **595**, A132 (2016)